

# Experimental Analysis of Thermal Runaway in 18650 Cylindrical Li-Ion Cells using an Accelerating Rate Calorimeter

*B. Lei, W. Zhao, C. Ziebert, A. Melcher, M. Rohde, H. J. Seifert*

*Institute of Applied Materials - Applied Materials Physics, Karlsruhe Institute of Technology, Germany*

## Abstract

In this work commercial 18650 lithium-ion cells with  $\text{LiMn}_2\text{O}_4$  cathode were exposed to external heating in an Accelerating Rate Calorimeter (es-ARC, THT Company) to investigate the thermal behavior under abuse conditions. New procedures for measuring external and internal pressure change of cells were developed. The external pressure was measured using a gas-tight cylinder inside the calorimeter chamber in order to detect venting of the cells. For internal pressure measurements, a pressure line connected to a pressure transducer was directly inserted into the cell. During the thermal runaway experiments, three stages (low rate, medium rate and high rate reaction) have been observed. Both pressure and temperature change indicated different stages of exothermic reactions, which produced gases or/and heat. The onset temperature of thermal runaway was estimated according to temperature and pressure changes.

## Introduction

To get rid of the dependence of petroleum and to reduce the  $\text{CO}_2$  emission, the best near-term solution for vehicles probably are electric (EV) and hybrid electric vehicles (HEV). However, for their extensive market penetration one of the most urgent requirements is to develop lithium-ion cells and batteries, which are safe and reliable even at higher temperatures. Several exothermic chemical reactions can occur inside a cell while the temperature rises. This may generate heat that accumulates inside the cell and accelerates the chemical reaction between the cell components, if the heat transfer to the surroundings is not sufficient. In this case, a thermal runaway can occur in consequence with leak, smoke, gas venting, flames etc., which leads to fire or explosion. To describe the thermal runaway one has to identify the main exothermic chemical reactions. According to (1-3) a thermal runaway can be described in four main steps:

- 1) At  $T > T_1$  the solid-electrolyte interface (SEI) decomposes in an exothermic reaction.
- 2) At  $T > T_2$  an exothermic reaction between the intercalated Li-ions and the electrolyte starts.
- 3) At  $T > T_3$  an exothermic reaction between the positive material and the electrolyte takes place under the evolution of oxygen inside the cell.
- 4) At  $T > T_4$  the electrolyte decomposes.

Jhu et al. (4, 5) studied thermal runaway characteristics (initial exothermic temperature, self-heating rate, pressure rise rate, maximum temperature and pressure) with vent sizing package 2, a commercially available accelerating rate calorimeter (ARC) manufactured by Fauske & Associates, LLC. This is a PC-controlled calorimeter with a pressure and temperature system that balances the internal and external pressure and temperature. The tested commercial batteries were considering two types of cathode materials, which were  $\text{LiCoO}_2$  and  $\text{Li}(\text{Ni}_{1/3}\text{Co}_{1/3}\text{Mn}_{1/3})\text{O}_2$  respectively. The maximum pressure  $P_{\text{max}}$  of  $\text{LiCoO}_2$  was 1.86 MPa, while for  $\text{Li}(\text{Ni}_{1/3}\text{Co}_{1/3}\text{Mn}_{1/3})\text{O}_2$  batteries it was only 1.13 MPa. With both cathode materials, high SOC levels aggravated the exothermic reactions. They also compared the self-heating behaviors of cells with different voltages by using the heat of reaction ( $\Delta H$ ), which was the product of mass of a cell, specific heat capacity of cells and the rise of temperature under adiabatic conditions (5). In addition, they built a model of self-heating rate of LIB from which the activation energy and frequency factor were determined and suggested that the self-heating rate increased exponentially with the temperature.

Golubkov et al. (6) made thermal runaway tests on batteries of  $\text{LiFePO}_4$  (LFP),  $\text{Li}(\text{Ni}_{0.45}\text{Mn}_{0.45}\text{Co}_{0.10})\text{O}_2$  (NMC) and LCO/NMC cathode materials by using a pressure-tight and airtight reactor, which was able to collect gases.  $\text{CO}$ ,  $\text{CO}_2$  and  $\text{H}_2$  represented about 80 % of the produced gases, and the others were  $\text{CH}_4$  and  $\text{C}_2\text{H}_4$ . The onset temperatures and released gas amounts of LFP, NMC and LCO/NMC were 195 °C and 50 mmol, 170 °C and 150 mmol, 150 °C and 270 mmol, respectively.

In this work, three kinds of experimental methods have been used to measure the temperature on the surface of the tested commercial 18650 cells, the pressure change due to released gases and the pressure change in re-sealed cells. The correlation between pressure and temperature behavior of lithium ion cells can characterize the degree of violence of a thermal runaway (4), and is very helpful in defining the threshold and stages of thermal runaway and the different reactions during thermal runaway.

## Experimental

For commercial 18650 lithium-ion cells with  $\text{LiMn}_2\text{O}_4$  (LMO) cathode three different thermal runaway testing methods have been used in an accelerating rate calorimeter (es-ARC, THT Company, s. Figure 1). The calorimeter chamber with a diameter of 10 cm and a height of 10 cm has one heater and one thermocouple located in the lid and bottom, respectively and two heaters and thermocouples (all type N) in the sidewall. The cell under study is fixed on the lid of the calorimeter as shown in Figure 1. The calorimeter temperature is controlled by a main or so-called bomb thermocouple fixed onto the surface of the cell. The heaters adjust the required temperatures depending on the measurement conditions. A steel casing outside serves as a protection. In the first method, only temperature and temperature rate were recorded (Figure 1). The standard *Heat-Wait-Seek* (HWS) method was applied for all measurements. The procedure is shown in Figure 3. The HWS method starts at 25 °C in the *Heat* mode by heating up the cell in small temperature steps of 5 °C (see Figure 2). At the end of each temperature step the *Wait* Mode is activated for 15 min to reach thermal equilibrium. After reaching thermal equilibrium, the system enters *Seek* Mode, which seeks the temperature rate and ends with two possible modes — *Exotherm* Mode or

*Heat Mode*. The decision is related to the selected *Temperature Rate Sensitivity* of 0.02 °C/min. If the measured temperature rate is larger than this value, the system goes into *Exotherm Mode*.

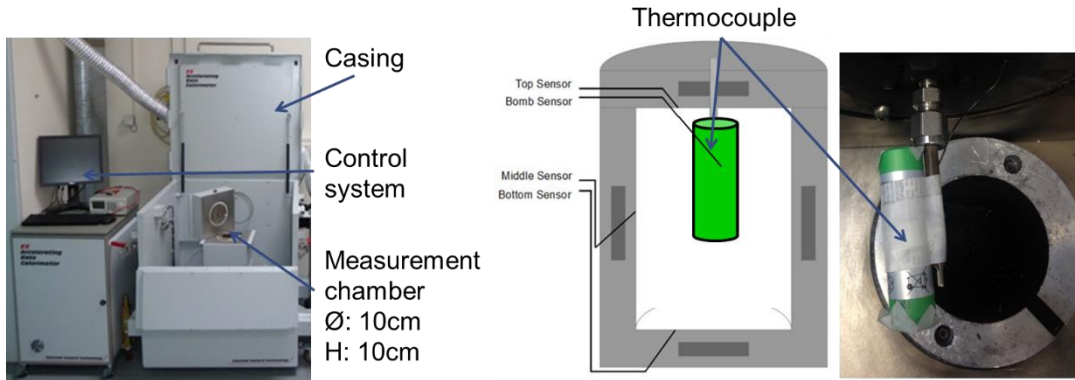


Fig. 1: Accelerating rate calorimeter (es-ARC) and setup of the cell in the ARC.

This mode provides an adiabatic environment, which means that no heat exchange between the sample and the surroundings is possible, so that the heat energy of reactions can be monitored by the measured temperature. On the other hand, if the temperature rate is smaller, the system goes back into *Heat Mode*. If the temperature exceeds the *End temperature* value of 250 °C, the ARC switches off the heaters and starts to cool down by introducing pressurized air to the calorimeter chamber.

The second method used an additional cylinder chamber for external pressure measurements (see Figure 3). The thermocouple was passed through a well-sealed hole and a pressure line connected with a pressure sensor was screwed on the cylinder chamber. It was very critical to screw every part of the cylinder chamber extremely tight to prevent for leaks. Similar to the adiabatic environment, the seal condition helped to monitor the external pressure change.

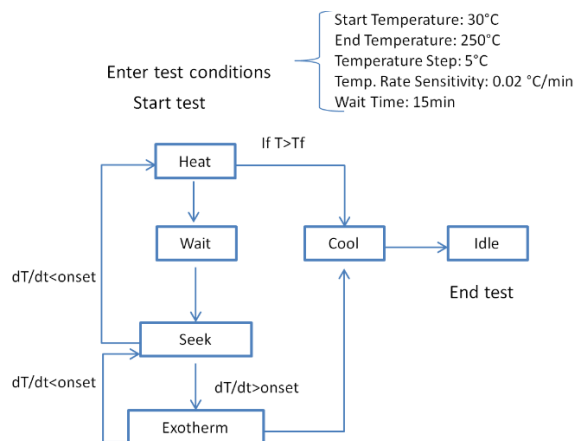


Fig. 2: Process of heat-wait-seek (HWS) method.

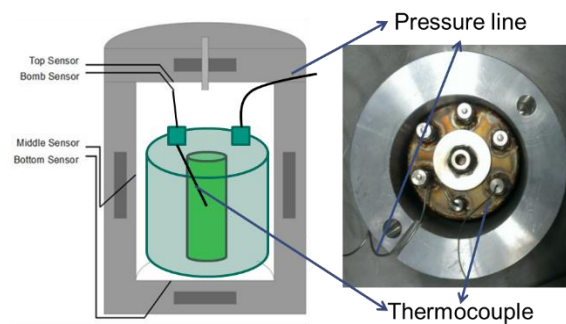


Fig. 3: External pressure measurement setup.

In contrast to the external pressure measurement, where the capillary leading to the pressure sensor was connected to the cylinder, in the third method this capillary was directly introduced into the functional cell for internal pressure measurements (Figure 4). Therefore, a suitable place had to be found by using images from X-ray tomography. X-ray tomography was conducted at the IAM X-Ray Imaging Laboratory at KIT. X-ray micro-tomography scans were performed on the cell using a Phoenix v/tome/x s system (Phoenix X-ray, GE Measurement and Control, Germany). The battery was rotated  $360^\circ$  about its long axis whilst 1600 projections were captured with the microfocus tube operating at 200 kV and 370(230)  $\mu\text{A}$ . The sample and detector were positioned in projection magnification providing an effective voxel size of 75(48)  $\mu\text{m}$  for the high resolution imaging. Tomography scans of the full cell were obtained, and subsequent 3D analysis of the reconstructed image data was performed using VG studio max software (Volume Graphics Company, Germany). Figure 4 shows as an example a 3D rendering of the tomographic data set for the 18650 cell with LMO cathode. The spirally wound internal structure of the cell and the hollow central section are clearly visible and on the top also the safety valve can be seen. It turned out that the best position for the pressure line is situated on the base of the cell, in the center of the hollow section, where a small hole was drilled and then a 1/16-inch diameter capillary was inserted. Then the cells have been resealed with epoxy resin. The described preparation procedure was performed in a Argon-filled glovebox, because the cell components are very sensitive to moisture.

Before the thermal runaway tests, the capacity of the cells was determined by three full cycles and finally they were fully charged to state of charge 100 % (SOC100), because this is the most critical condition for Li-ion cells according to (7). The method of charge was CC/CV. Which means that firstly the cell is charged at constant current at 1C rate (CC) up to the maximal voltage, and then it is charged at constant voltage (CV) with decreasing current until the current reaches 10 % of its starting value.

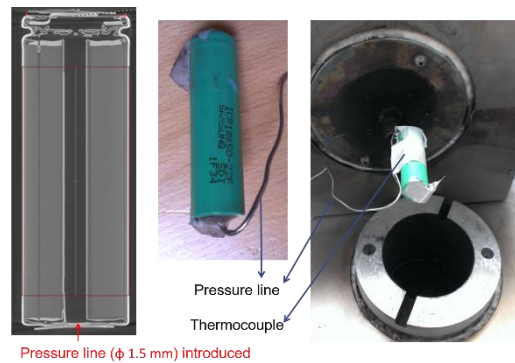


Fig. 4: Setup for internal pressure measurement.

## Results and Discussion

In the following the three different test methods will be demonstrated for the cell with LMO cathode. Figure 5 compares the time evolution of the measured surface temperatures for the three different methods and three identical cells at SOC100. From this figure, it is easily to distinguish the *Heat-Wait-Seek* periods and the *Exotherm* periods. At temperatures below about 80 °C, the temperature curve increased with steps of 5 °C. Then a first exothermic reaction can be seen. Afterwards, the system went back to heat mode at 100 °C, and the HWS mode was active until 110 °C. Then the temperature went up continuously in *Exotherm* mode until thermal runaway happened.

So three stages were observed in the thermal runaway tests, which were assigned according to the literature (1-3) to:

- 1) At about 80 °C solid electrolyte interface (SEI) decomposed.
- 2) At about 110 °C an exothermic reaction between embedded Lithium ions and electrolyte started, which resulted in the reduction of electrolyte at the negative electrode.
- 3) At about 200 °C an exothermic reaction between active positive material and electrolyte at positive electrode took place.

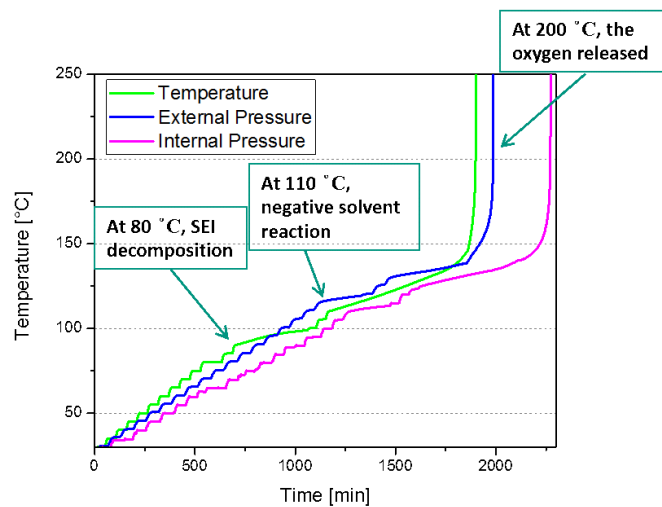
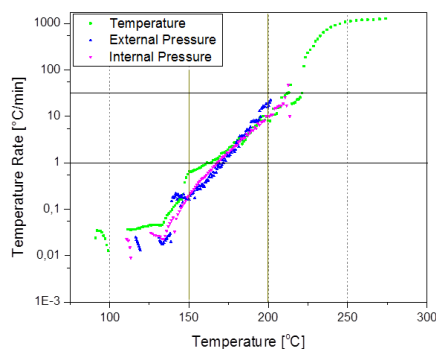


Fig. 5: Comparison of temperature curves vs. time measured by different methods.

When comparing the three curves, the time until the thermal runaway is reached increased from the only temperature via the external up to the internal pressure measurements. The reason is that the system needs to heat up the cylinder for the external pressure tests and that some heat loss occurs via the pressure line during internal pressure tests. Even though the three curves do not perfectly overlap each other, however, the tendencies are the same. We can have a more specific view using Figure 6 a), which shows the temperature rate vs. the temperature. Here the three stages can be distinguished more easily and the measured temperature rates agree well with each other for all three test methods.

a)



b)

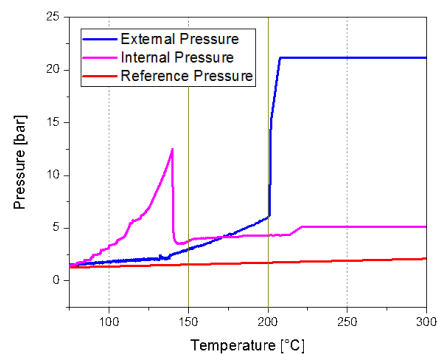


Fig. 6: a) Comparison of temperature rate vs. temperature curves measured by different methods.  
b) Compare pressure vs. temperature by different methods.

In the temperature region 80 °C to 150 °C, the temperature rate is lower than 1 °C/min. From 150 °C to 200 °C, the energy was released with medium rate lower than 25 °C/min. Above 200 °C, the exothermic reactions happened in a violent way with a temperature rate over 1000 °C/min.

Finally, in order to correlate temperature and pressure measurements the pressure values taken from the external and the internal pressure tests are plotted vs. the temperature in Figure 6 b). The additional red line represents the expansion of the air with increasing temperature according to the ideal gas law. For the external pressure measurement, the difference between the measured blue line and the red line can be regarded as the amount of gases that come from the leaking cell. As the temperature increased, the difference became larger and larger, showing that more and more gases were produced. There was a gas leaking from 80 °C and produced gases were released into the cylinder, because of exceeding the threshold pressure of the safety valve. At 130 °C, the difference became larger. At 200 °C, which is also the start temperature point of stage 3, the difference was significant. For the internal pressure measurement, starting at 80 °C, the difference was increasing continuously, indicating the beginning of gas production and SEI layer decomposition. Between 130 °C and 140 °C, the valve of the battery opened and gases were released.

Following the procedure described by Golubkov et al. (6) the amount of produced gases was calculated from the measured external pressure. The cell with LMO cathode released 76.5 mmol gases during thermal runaway. Golubkov et al. reported that 18650 cells with LCO/NMC cathode material released gases of 265 mmol, and those with pure NMC 149 mmol. This comparison indicates a better exothermic stability of the LMO cathode.

## Conclusions

Three stages have been observed in thermal runaway tests with 18650 Li-Ion cells with LMO cathode by correlating temperature and pressure curves. The first stage began with gases production at about 80 °C. The reaction in the first stage was likely to be the SEI layer decomposition. The onset temperature was about 113 °C, when the second stage started; from this temperature, the cells started self-heating until the thermal runaway. In future studies, it could be interesting to confirm all these stages exactly and analyze produced gases and material components after thermal runaway using post-mortem analysis by opening the cells after the experiment has been stopped at the different stages. The next step could be to use the derived thermokinetic parameters as input parameters for our coupled electrochemical thermal model (7), which encompasses a simple combustion model coming from reaction kinetics including various types of heat sources based on an Arrhenius law.

## Acknowledgements

This R&D project is part of the project IKEBA which is funded by the Federal Ministry for Education and Research (BMBF) within the framework “IKT 2020 Research for Innovations” under the grant 16N12515 and is supervised by the Project Management Agency VDI | VDE | IT. The authors would like to express their gratitude to A. Maier, IAM-AWP, for recording the X-Ray tomography images.

## References

- [1] E. P. Roth, D.H. Doughty, *J. Power Sources*, **128**, 308 (2004).
- [2] R. Spotnitz, J. Franklin, *J. Power Sources*, **113**, 81 (2003).
- [3] D. P. Abraham, E.P. Roth, R. Kostecki, K. McCarthy, S. MacLaren, D.H. Doughty, *J. Power Sources*, **161**, 648 (2006).
- [4] C.-Y. Jhu, Y.-W. Wang, C.-Y. Wen, C.-M. Shu, *Applied Energy*, **100**, 127 (2012).
- [5] C-Y. Jhu, Y.-W. Wang, C.-M. Shu, J.-C. Chang, H.-C. Wu, *Journal of Hazardous Materials*, **192**, 99 (2011).
- [6] A. W. Golubkov, D. Fuchs, J. Wagner, H. Wilsche, C. Stangl, G. Fauler, G. Voitic, A. Thaler, V. Hacker, *Journal of RSC Advances*, **4**, 3633 (2014).
- [7] A. Melcher, C. Ziebert, M. Rohde, B. Lei, H.J. Seifert, *Energies*, **9** 292 (2016), doi:10.3390/en9040292.